Phosphosulfide semiconductors for optoelectronics and solar energy conversion

Lena A. Mittmann[1] and Andrea Crovetto[1*]

[1] National Centre for Nano Fabrication and Characterization (DTU Nanolab), Technical University of Denmark, 2800 Kongens Lyngby, Denmark

E-mail: ancro@dtu.dk

Abstract

Inorganic phosphosulfides – materials containing phosphorus, sulfur, and at least one metal – are a vast and chemically-versatile family of materials. Benefiting from a wide range of possible phosphorus oxidation states, phosphosulfide semiconductors exist as thiophosphate compounds with various types of P-S polyanions, as genuine multi-anion compounds with or without P-P bonds, as solid solutions, and as many intermediate cases. Since metal phosphides and metal sulfides are among the highest-performing optoelectronic semiconductors, it seems reasonable to consider the phosphosulfide family as a potential pool of materials for solar cells, photoelectrochemical cells, and light-emitting diodes. Nevertheless, phosphosulfide semiconductors have very rarely been characterized with these applications in mind. In this Perspective, we reflect on the potential applicability of known and hypothetical phosphosulfides as light absorbers and emitters in optoelectronic devices. First, we distill the existing knowledge accessible through the Materials Project database, finding promising phosphosulfides among the compounds already present in the database, and identifying what we see as the general advantages and challenges of phosphosulfides as optoelectronic materials. Then, we propose three concrete research directions aimed at finding novel high-quality phosphosulfide semiconductors with high light absorption coefficients, high carrier mobilities, and long carrier lifetimes. In particular, we argue that the versatility of phosphorus in this class of materials could potentially be exploited to engineer defect tolerance. Finally, we devise and describe a custom synthesis setup dedicated to high-throughput exploration of thin-film phosphosulfides.

Keywords: Phosphides, sulfides, multi-anion semiconductors, solar cells, water splitting, light-emitting diodes, optoelectronic properties, materials discovery

1. Introduction

Optoelectronic energy conversion is very likely to be a key technology for a sustainable energy future. This broad field encompasses photovoltaics (PV, sunlight-to-electricity conversion), photoelectrochemistry (PEC, sunlight-to-fuel conversion through electronic processes), and light emitting diodes (LEDs, electricity-to-light conversion). All these technologies are based on similar fundamental processes: Light absorption and emission, electron-hole separation and recombination, and their transport to/from electrode materials. Although technology-specific requirements exist, PV, PEC, and LEDs exhibit a common thread. They all require a semiconductor material combining a high light absorption coefficient α, long photocarrier lifetimes τ, and high photocarrier mobilities μ.[1–3] For simplicity, we will refer to such ideal materials as "high-quality semiconductors" throughout this paper. Current materials research efforts in this field are especially targeted at the discovery and development of semiconductors with relatively wide band gaps, often above 1.5 eV. The main reason is the lagging performance of wide band gap sub-cells in cost-effective multi-junction PV and PEC technologies,[4] as well as the location of the low-photon-energy edge of the visible region in LEDs (around 1.6 eV).

The development of new inorganic semiconductors has often been driven by charge-neutral elemental substitutions in already-known semiconductors.[5] Even though these substitutions could be applied on either the cation sites or on the anion sites, history has given a strong preference to the cations, generally leading to the development of multi-cation

semiconductors. A well-known example is the substitution starting from CdS to $CuInS_2$ and further to Cu_2ZnSnS_4.[6] The PV field is full of multi-cation materials, such as the inorganic halide perovskite $CsPbI_3$ and various other ternary absorbers such as $ZnSnN_2$ and $AgBiS_2$.[6,7]

Well-established semiconductors such as $InAs_xP_{1-x}$ and $CuIn_{1-x}Ga_xS_ySe_{2-y}$ are often synthesized with more than one anion. However, these materials are not genuine multi-anion compounds but rather anion solid solutions, in which both anions occupy the same crystallographic sites with different fractional occupancies. In these cases of anion solid solutions, the properties of, say, $InAs_xP_{1-x}$ can be predicted with reasonable accuracy from those of the InAs and InP binaries using Vegard's law.[8,9] Solid solutions are useful for fine-tuning the properties of their constituent binaries, such as lattice parameters and band gaps. However, unique or unexpected properties are rare. This behavior is in stark contrast with the genuine multi-cation semiconductors mentioned in the previous paragraph. These are unique compounds where each cation occupies a specific crystallographic site. Hence the properties of $CsPbI_3$ are unique, instead of simply being a weighted average of the properties of CsI and PbI_2. With the additional degree of freedom given by the extra cation, $CsPbI_3$ turns out to be an excellent PV absorber, even though CsI and PbI_2 are not.

In contrast to the multi-cation case, experimental investigations of genuine multi-anion materials for optoelectronic energy conversion are much more sparse.[10] There has been some experimental work on certain oxynitrides (e.g., $LaTiO_2N$, TaON [2,10,11]), oxysulfides (e.g., $Y_2Ti_2O_5S_2$ [11], oxyhalides (e.g., BiOI [11]) and sulfoiodides (e.g., SbSI [12]). However, very few multi-anion materials have been explored and their PV efficiencies are generally below 5%.[13]

In this Perspective, we will discuss the prospects of multi-anion and polyanionic phosphosulfides (PSs) as potential high-quality semiconductors. We will see that PSs are still nearly unexplored in the context of optoelectronic energy conversion. Nevertheless, most of the known PS materials feature band gaps in the visible, crystal structures with three-dimensional bonding networks, and a remarkable degree of chemical diversity that is not easily matched by other inorganic material families. The fundamental reason for their chemical versatility is the wide range of oxidation states that phosphorus can take in the simultaneous presence of a more electropositive element (a metal) and a more electronegative one (sulfur). The implications for the discovery of optoelectronic semiconductors are intriguing. In fact, it is already possible to identify PSs with direct band gaps in the visible and low carrier effective masses – potential indicators of high α and high μ – when phosphorus is both in its maximum (+5) and minimum (-3) oxidation state. We will conclude this Perspective by proposing an approach for the high-throughput synthesis of known and hypothetical PS compounds in thin-film form.

2. Review of previous work

2.1 General features of phosphosulfides

The generic case of an inorganic material containing phosphorus, sulfur and at least one metal in any stoichiometry and structure will be referred to as phosphosulfide (PS) in this paper. Judging from the number of compounds present in the Materials Project (MP) database[14], PSs have received less attention than oxygen-containing multi-anion materials. Nonetheless, they are among the non-oxide multi-anion families with the most entries (Fig. 1a). The "synthesised" bar refers to materials that have also been synthesised in bulk form according to the ICSD database.[15]

The known PS materials can crystallize in a wide variety of structures, in which the overall structural dimensionality (i.e., the dimensionality of the network of chemical bonds in the material) can be 3D, 2D, 1D, or 0D. [16–20] In this paper, we will always refer to the structural dimensionality – rather than the thickness – when labeling PS materials as 3D, 2D, 1D, or 0D. PS compounds generally do not react with moisture or oxygen, except for at the surface. [21–30] An exception is PSs with high alkali metal content, which are often reported to be hygroscopic.[20] Various PSs are also reported to be stable in electrolyte solutions under a wide range of pH values.[31] Thus, PSs are not intrinsically air-sensitive materials.

Phosphosulfides with P/S < 1. A closer look at the known PSs indicates that they mainly consist of ternary and quaternary compositions, and that the preferred (molar) stoichiometric P/S ratios are 1, 1/3, 2/7 and 1/4, (Fig 1b). PSs exhibiting the 1/3, 2/7 and 1/4 ratios are usually called thiophosphates, due to their similarity to their oxide-based counterparts (phosphates). Rather than being true multi-anion materials, thiophosphates are polyanionic compounds in which P and S form a well-defined structural unit (the polyanion) with P in the center. The metal cations only bond to the S atoms of the polyanions, and therefore P is in a positive oxidation state, as it tends to donate electrons to S within the polyanion (Fig. 1c) (visualized with VESTA [32]). This is a completely opposite behavior with respect to the well-known III-phosphide semiconductor (In,Ga)P, and also to other emerging phosphide semiconductors such as $ZnGeP_2$ and CuP_2.[33,34] In these single-anion semiconductors, P is always in a negative oxidation state (usually -3, unless P-P bonds are present). Instead, thiophosphates have more similarities with polyanionic semiconductors based on other elements, such as the well-studied PEC material $BiVO_4$.[2]

The most common polyanions in thiophosphates are $[PS_4]^{3-}$ in materials with P/S = 1/4 such as Cu_3PS_4; $[P_2S_6]^{2-}$, and $[P_2S_6]^{4-}$ in materials with P/S = 1/3 such as KPS_3 and $NiPS_3$; and $[P_2S_7]^{-4}$ in materials with P/S = 2/7 such $Ag_4P_2S_7$.[20]

These polyanions are shown in Fig. 1c. In all these cases except for $[P_2S_6]^{4-}$, each phosphorus atom is tetrahedrally coordinated to four sulfur atoms. The polyanions simply differ by the number of shared S atoms between pairs of tetrahedra (no sharing in $[PS_4]^{3-}$, corner-sharing in $[P_2S_6]^{2-}$, and edge-sharing in $[P_2S_7]^{-4}$). The $[P_2S_6]^{4-}$ polyanion can still loosely be visualized as two linked tetrahedra, but with a P-P bond rather than S atoms as the link. In all these thiophosphates, P is in the +5 or +4 oxidation state (Fig. 1c).

Phosphosulfides with P/S = 1. The non-thiophosphate compounds with P/S = 1 in the MP database are an intermediate case between the two extremes of "textbook" P-S polyanions and separate P and S anions that are independent of each other. A common anionic motif is a simple P-S bond

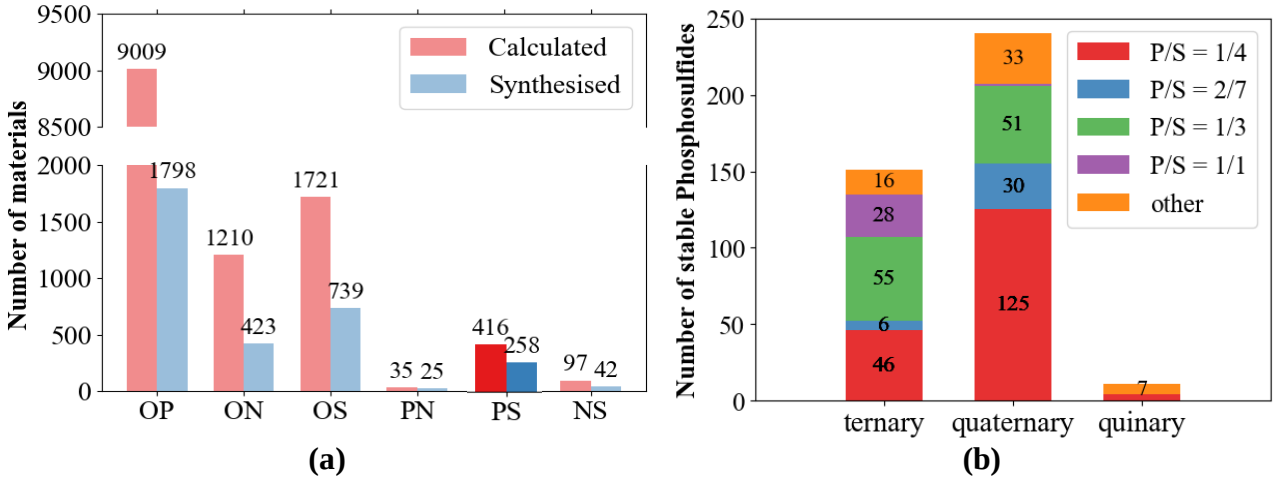

P/S ratio	P/S = 1/1		P/S = 1/3		P/S = 2/7	P/S = 1/4
Polyanion	$[PS]^{-x}$	$[P_2S_2]^{-x}$	$[P_2S_6]^{-4}$	$[P_2S_6]^{-2}$	$[P_2S_7]^{-4}$	$[PS_4]^{-3}$
Known P oxidation states	-1, -3	-2	+4	+5	+5	+5
Structure	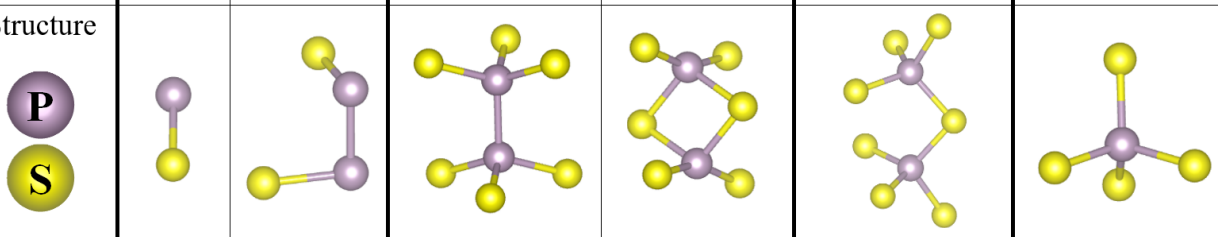					
Bonds	P-S M-S M-P	P-P P-S M-S M-P	P-P P-S M-S	P-S M-S	P-S M-S	P-S M-S

(c)

Figure 1. ***a)*** *Number of unique compounds available in the Materials Project (MP) database [14] among materials containing two anions among O, P, N, S, and an arbitrary number of metals. The "synthesised" bar refers to materials that have also been synthesised in bulk form according to the ICSD database [15].* ***b)*** *Number of unique, thermodynamically stable PSs available in the MP database, grouped by number of elements and coloured by anion stoichiometry. Throughout this paper, "stable" means that the energy above the calculated stability hull (E_{hull}) is lower or equal to 0.2 eV.* ***c)*** *Summary of general features found in PSs grouped by the anion stoichiometry including the formula of the most common polyanions, the known oxidation states of phosphorus in these polyanions, their structure represented as a ball and stick model visualized with VESTA [32] and the bonds found in the materials with the respective anion ratio.*

(as in FePS), or two P-S bonds linked by P-P bonds (as in PdPS). Unlike the case of thiophosphates, here P participates in bonding with the metal cations, so it typically appears in intermediate oxidation states (-1 or -2). Among the known compounds with P/S = 1, there are also cases where P-S bonds are completely absent and only metal-S and metal-P bonds exist as in conventional multi-anion materials like oxynitrides or oxyhalides. In these cases (such as YPS and TaPS) the P oxidation state can be between -3 and -1, depending on whether P only bonds to metal atoms or also to other P atoms.

Phosphosulfides with P/S > 1. To the best of our knowledge, PSs with a P/S ratio above 1 have never been synthesized and are rarely present in computational materials databases. The only such material available on MP seems to be Zr_2P_3S. Nevertheless, a 2019 computational screening study by Amsler et al. [35] based on density functional theory (DFT) included four PSs with P/S = 2 in their pool of candidates (Mg_4P_2S, Ca_4P_2S, Sr_4P_2S, and Ba_4P_2S). Unexpectedly, the authors found all these compounds except for Mg_4P_2S to be thermodynamically stable in a previously unknown crystal structure derived from the Ba_3As_2 structure. The implications of this recent discovery on optoelectronic energy conversion applications will be discussed later. At this stage, we simply note that the results by Amsler et al. suggest that a large portion of the PS material space (i.e., compounds with P/S > 1) may still be awaiting discovery.

2.2 Common applications of phosphosulfides

Several PS materials have demonstrated high technological value and/or unique properties not found in other groups of materials. For example, $Li_{10}GeP_2S_{12}$ demonstrated record ionic conductivity in 2011 and Li-based thiophosphates are among the most promising solid electrolytes for solid-state batteries;[36] in 2020, $CuInP_2S_6$ was found to be a ferroelectric material with exotic features;[37] and in 2020, unique excitonic effects were found in atomically-thin, antiferromagnetic $NiPS_3$.[38] In general, thiophosphates with 3D structural dimensionality have predominantly been investigated as solid electrolytes for Li and Na batteries[39] and as non-linear optical materials.[40] Thiophosphates with 2D structural dimensionality (often referred to as "van der Waals" materials) have mainly been studied in the fields of Li and Na battery electrodes [41–44], ferroelectrics [45–47], magnetic materials[16,17,48–50], and catalysts for the oxidation of S^{2-} [51], the reduction of CO_2 [52], the HER [26,53–57] and the OER [24,29,57].

Conversely, only few papers report on optoelectronic characterization of PS semiconductors.[30,35,58–66] Even when such characterization is presented, the samples are generally synthesized in bulk form (crystal or powder) or as nanoparticles. This has so far prevented the fabrication of solid-state devices, such as solar cells and LEDs. PSs in thin-film form, which would be particularly advantageous for optoelectronic applications, are almost absent from the literature. In the following section, we will review the few studies involving PS in the context of optoelectronic energy conversion.

2.3 Previous studies on phosphosulfides for optoelectronics

The only computational study investigating an appreciable range of PS semiconductors for optoelectronic applications is the DFT screening study by Han and Ebert.[58] The authors considered 18 ternary thiophosphates with a MPS_3 (M = Na, K, Rb, Cs, Cu, Ag), MPS_4 (M = B, Al, Ga, In, Sb, Bi) and M_3PS_4 (M = Li, Na, K, Rb, Cu, Ag) composition. All these compounds are based on the tetrahedral $[PS_4]^{3-}$ or $[P_2S_6]^{2-}$ polyanions but have different crystal structures. Band gaps between 1.7 and 4.1 eV were determined with the state-of-the-art HSE06 functional.[67] Many of the investigated materials had sufficiently low carrier effective masses to be considered for optoelectronic applications where electronic transport matters. Na_3PS_4 revealed high p-type dopability, a band gap above 3 eV and a low hole effective mass, making it a potential p-type transparent conductor. Ag_3PS_4 was identified as the most promising PV absorber in the study, due to a direct band gap in the visible and lack of deep defects with a low formation energy. Since the band alignment of Ag_3PS_4 with the water redox potentials was found to be favorable, Ag_3PS_4 was also suggested as a potential PEC water splitting absorber. Both Na_3PS_4 and Ag_3PS_4 are 3D PSs.

Some of the thiophosphates screened by Han and Ebert have been experimentally investigated. Tiwari et al. studied the optoelectronic properties of $BiPS_4$ powders for solar energy conversion.[59] $BiPS_4$, a 3D PS, was found to have a direct band gap of 1.72 eV, n-type conductivity, moderate electron effective masses, and an encouraging carrier lifetime around 1 ns.[59] Shaddad et al. utilized a $BiPS_4/BiVO_4$ heterojunction to increase the photocurrent of a bare $BiVO_4$ photoanode for PEC water splitting.[26]

The $Cu_3PS_{4-x}Se_x$ solid-solution series (3D) was synthesized in powder form by Itthibenchapong et al., and investigated as a potential PV absorber.[60] With increasing sulfur content, the band gap increased from 1.35 eV (Cu_3PSe_4) to 2.38 eV (Cu_3PS_4). This band gap range covers the requirements of many optoelectronic energy conversion technologies. [60] Spectrally narrow photoluminescence close to the band gap energy and a PEC response were subsequently measured for pure-sulfide Cu_3PS_4 nanoparticles,[61] which were also employed as a hole transport layer in perovskite solar cells.[30]

The optoelectronic properties of the 2D PS $GaPS_4$ were computationally investigated by two groups. Liu et al. predicted a reduction of the band gap and improved band alignment for unassisted PEC water splitting upon

introduction of single transition metal atoms into $GaPS_4$.[57] Shen et al. performed defect calculations in $GaPS_4$ to derive favorable growth conditions for n- and p-type doping.[62] Furthermore, they found that a higher optical band gap in $GaPS_4$ compared to the fundamental calculated band gap is due to dipole-forbidden transitions. This feature was independently found in Ag_3PS_4,[58] despite the substantially different structures in the two compounds. $Pd_3(PS_4)_2$, another 2D PS material with $[PS_4]^{3-}$ anions, was experimentally studied by Roy et al., who reported a PEC response from exfoliated nanosheets of this material.[53]

A few 2D thiophosphates with $[P_2S_6]^{4-}$ anions have also been optoelectronically characterized to a limited extent. In 1979, Brec et al. characterized MPS_3 crystals and powders (M= Mn, Fe, Ni, Zn, Cd, $In_{0.66}$)[63] and reported their band gaps (1.5-3.5 eV), electrical resistivity (10^2-10^4 Ωcm) and α (exceeding 10^4 cm^{-1} just above the fundamental band gap). These materials were also computationally examined by Zhang et al. for PEC applications.[64] The authors calculated their band alignment and optical absorption coefficient, and concluded that $FePS_3$ and $NiPS_3$ exhibited a promising combination of properties for PEC water splitting. Cropek et al. characterized two different phases of Ag_2PS_3 with 3D structural dimensionality. [66] Both phases were found to be air-stable, n-type semiconductors with indirect band gaps of 2.5 eV and detectable PEC responses. After the discovery of ferroelectricity in $CuInP_2S_6$,[37] Li et al. reported the bulk photovoltaic effect in single crystals and exfoliated flakes of this 2D quaternary thiophosphate featuring the $[P_2S_6]^{4-}$ polyanions.[65] Wang et al. employed exfoliated $CuInP_2S_6$ sheets in PEC cells, and observed an increased photocurrent when oxygen was incorporated on the $CuInP_2S_6$ surface.[55]

We could only find a single, very recent study on the optoelectronic properties of a $[P_2S_7]^{4-}$ thiophosphate (Feng et al. [54]). Using first-principles calculations, the authors concluded that two different phases of $Ag_4P_2S_7$ possess high α in the visible and suitable band edge positions for PEC water splitting.[54] Moving to non-thiophosphate PSs with P/S = 1, Roy et al. demonstrated working photodetectors based on exfoliated PdPS sheets.[25] Houari and Benissad suggested CoPS as a PV absorber based on first-principle calculations.[68]

As mentioned in Section 2.1, it appears that no materials with P/S > 1 have been synthesized in any form. However, the

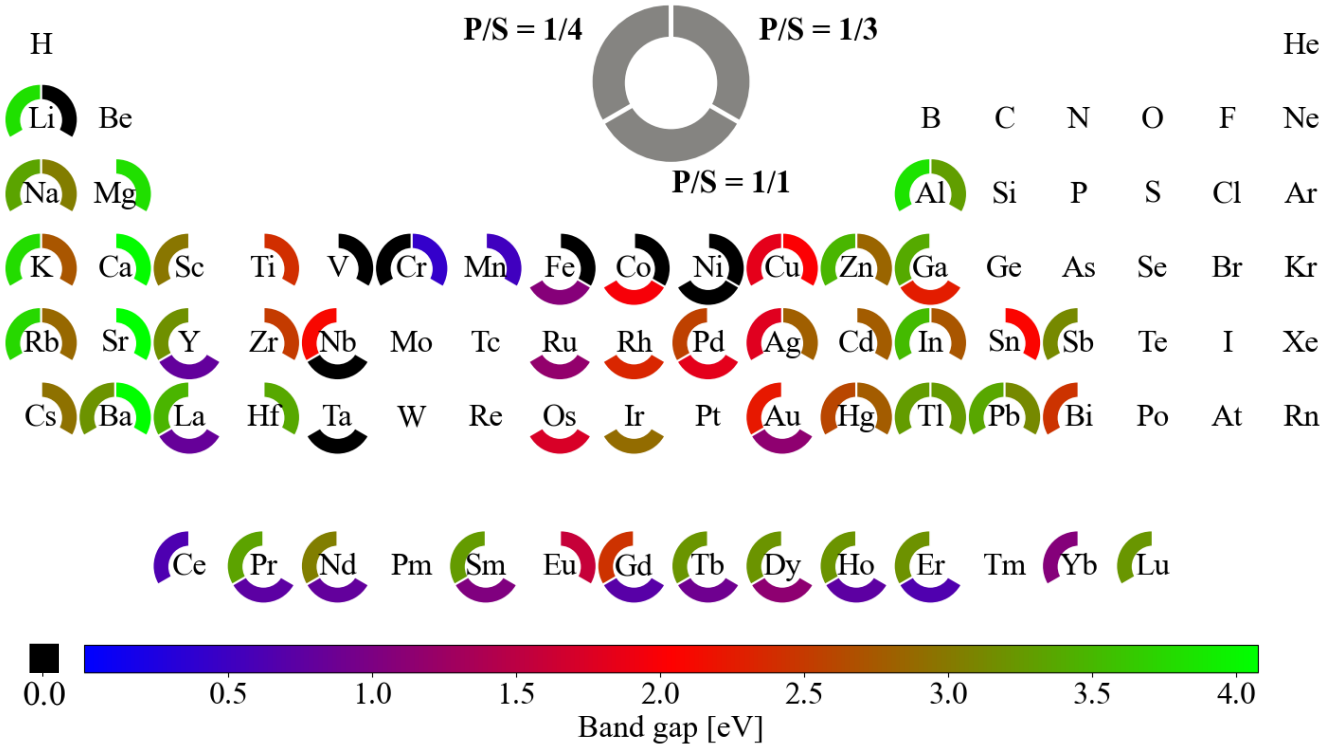

Figure 2. Calculated band gaps for the most stable (i.e., lowest E_{hull}) ternary PS for each metal cation and each P/S ratio of 1/1, 1/3, and 1/4. Only materials with $E_{hull} \leq 0.2$ eV are considered. For two materials with equal stoichiometry and E_{hull}, preference is given to the one with a band gap closer to 2 eV. The band gaps include a correction to the PBE-level band gaps [69] available on the MP database, to account for their systematic underestimation. The corrected values are obtained by polynomial regression between the PBE band gaps and the more accurate band gaps calculated at the HSE06 level [70] on a sample of 62 PSs available in the SNUMAT database [71]. More details are explained in the SI. The position in the periodic table indicates the third constituent element of each PS. Metallic compounds (band gap of 0) are displayed in black.

recent computational screening study by Amsler et al. suggests that some of these hypothetical P-rich compounds may have very promising properties for optoelectronic applications. The authors investigated ternary compounds with a X_4Y_2Z stoichiometry, where X =Mg, Ca, Sr, Ba; Y =P, As, Sb, Bi; and Z=S, Se, Te.[35] The study included machine-learning prediction of stable stoichiometries, global structure prediction, and detailed DFT calculations of the hypothetical materials that resulted from the first two steps. Three out of four phosphosulfides (Ca_4P_2S, Sr_4P_2S, and Ba_4P_2S) were found to be on the convex stability hull in their lowest-energy structure. Thus, these materials are likely to be synthesizable. All three materials exhibited a direct band gap at the Γ point and high band edge dispersion (i.e., low effective masses). The former is often correlated with a high α, the latter with high μ. Their band gaps were found to decrease when moving down the group. At the PBE level, Ca_4P_2S had a band gap of 1.8 eV and Ba_4P_2S had a band gap of 1.3 eV. At the HSE level (known to yield more accurate band gaps), the corresponding band gaps were roughly 2.7 eV and 2.0 eV, respectively. These combined features indicate that these newly discovered PSs could be highly interesting for visible light emission, multijunction solar cells, and PEC water splitting applications.[35] Their potential air sensitivity should, however, be investigated.

3. Semi-quantitative screening of the known ternary phosphosulfides

We have seen that some PSs have been studied for their optoelectronic properties, but only very few materials have been reported in more than a single publication. In addition, work has almost only focused on thiophosphates. Does the PS material family warrant a broader, rational search for new semiconductors? If so, where should we search? To help answer these questions, we examine selected properties of all the ternary PSs present on MP and predicted to be thermodynamically stable by DFT. The examined properties are band gap (Fig. 2), structural dimensionality (Fig. 3), and effective masses (Fig. 4). When specific materials are discussed, reference is made to their Materials Project ID.

3.1 Band gaps

The band gaps (calculated at the PBE level[69] and corrected to the HSE level[70]) of the lowest-energy ternary PS for each metal cation and the most common P/S ratios are displayed in Figure 2. See Supplementary Information for details on the correction and the data used from the SNUMAT database [71]. PSs span the whole range from metals to wide-gap insulators, but most of them are predicted to be semiconductors, often with band gaps in the visible. This is a promising trend for applications within optoelectronic energy conversion. Ternary PSs from s-block metals generally feature the widest band gaps followed by the ternaries incorporating p-block and Group 12 metals, while the PSs including d-block or f-block metals feature the lowest band gaps. For most metal cations, a P/S ratio of 1/1 generally yields the narrowest band gaps and a P/S ratio of 1/4 the widest band gaps.

3.2 Structural dimensionality

Although thiophosphates with 2D structural dimensionality have received particular attention,[16,21,31,72] data mining from the MP database reveals that most of the known PSs actually have 3D dimensionality (Fig. 3a). For quaternary and quinary PSs, the share of 3D-structured materials is even higher than what is found in ternary systems (Fig. 3a). Interestingly, most of the 2D-structured materials appear in

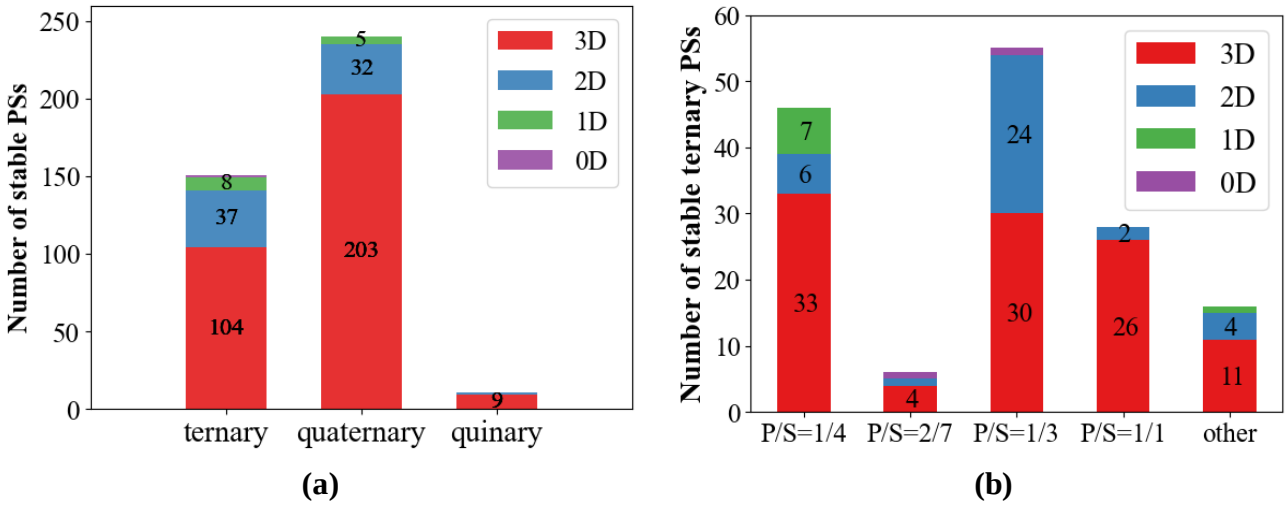

Figure 3. ***a)*** *The number of stable (E_{hull} ≤ 0.2 eV) ternary, quaternary, and quinary PSs available in the MP database grouped by structural dimensionality (0D, 1D, 2D, 3D).* ***b)*** *The structural dimensionality of the available stable ternary PSs grouped by P/S ratio with P/S ratios of 1/4, 2/7, 1/3, 1/1 and a summary of all others.*

the P/S = 1/3 category (Fig. 3b) in combination with the $[P_2S_6]^{4-}$ polyanion (Fig. 1c).

The predominance of 3D structures is encouraging for optoelectronic energy conversion application, because 3D structural dimensionality is usually a necessary (though not sufficient [73]) condition for good photocarrier transport in all directions. Specifically, 3D structures with high spatial- and energy overlap between the orbitals constituting their band edges usually result in high band dispersion and low effective masses of electrons and holes in all directions. Since μ is inversely related to the effective mass, low effective masses are usually correlated with high carrier mobilities. Indeed, all the inorganic PV absorbers with demonstrated efficiencies above 15% have 3D structural dimensionality.[74]

3.3 Effective masses

Along with the structural dimensionality, it is useful to extract quantitative values of the effective masses of the ternary PS semiconductors for which a band structure calculation is available on MP. The direction-averaged effective masses of holes and electrons (extrapolated using the BoltzTrap2 package [75,76]) in these PSs are displayed in Fig. 4. We find that a few compounds have low effective masses in both the valence and conduction band. Some examples are the previously identified Ag_3PS_4 (mp-12459), Cu_3PS_4 (mp-3934) and Na_3PS_4 (mp-28782), [58,60] the newly identified $Zr(PS_3)_2$ (mp-8203), as well as various narrow-gap compounds with d- and f-block metals.

However, at least one of the effective masses is greater than the rest mass of the electron m_0 in most of the known ternary PSs (Fig. 4). Therefore, the predominance of 3D structures in PSs is generally not sufficient to ensure high μ in this class of compounds. We also note that holes in PSs are generally heavier than electrons, as often seen in semiconductors. Since low effective masses are not fundamentally prohibited by low dimensionality in PSs, we argue that one of the key areas of research in PS semiconductors for optoelectronic energy conversion should be to identify design rules for obtaining low effective masses.

4. Searching for new phosphosulfide semiconductors

The analysis in the previous section indicates that it might be necessary to move beyond the already-known ternary PSs to find more than a handful of candidates for high-quality semiconductors. Assuming that PSs with band gaps in the visible are plentiful (Fig. 2), the key questions are where to

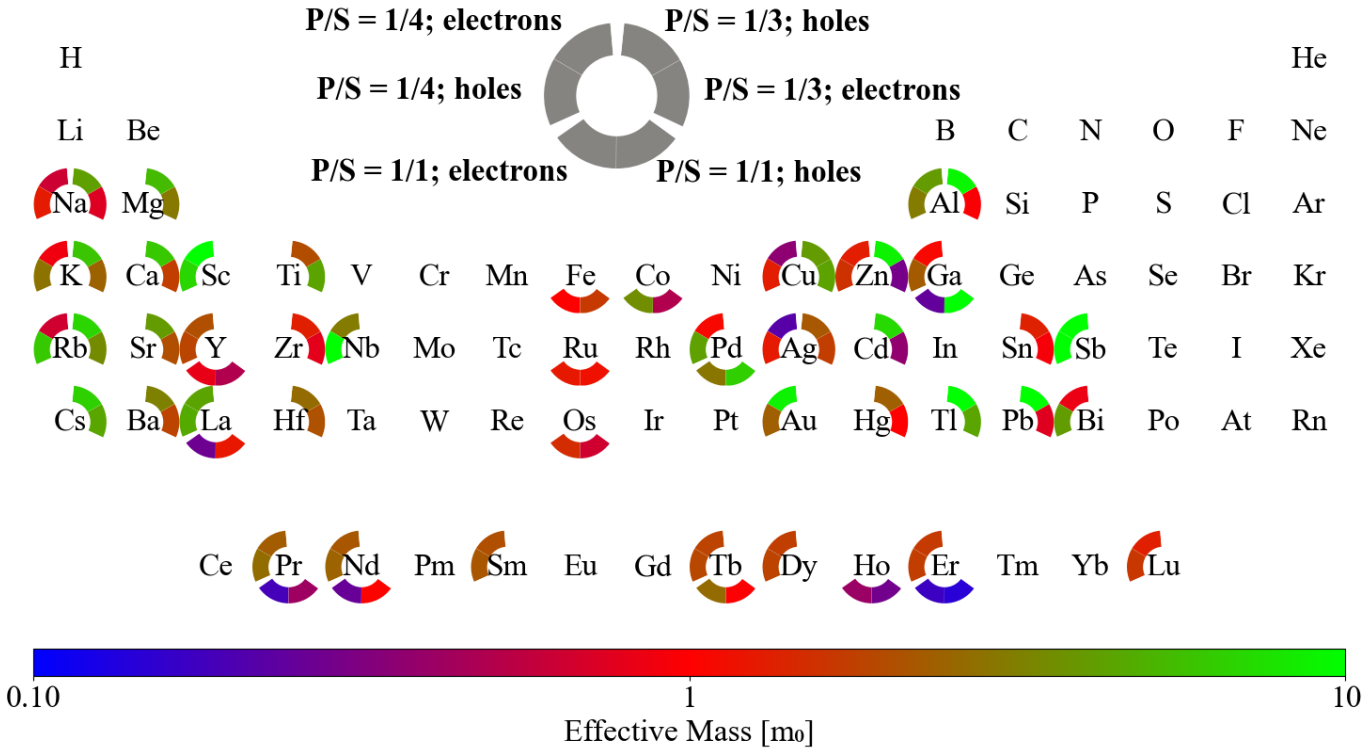

Figure 4. Calculated direction-averaged carrier effective masses for electrons and holes in the most stable ternary PSs (E_{hull} ≤ 0.2 eV) for each metal cation and each P/S ratio of 1/1, 1/3, and 1/4. Only materials with an electronic band structure calculation available on MP are considered. Thus, the materials shown here for each metal cation and P/S ratio do not always correspond to the ones shown in Fig. 2. In the case of two materials with equal stoichiometry and E_{hull}, preference is given to the one with the smaller sum over the effective masses of both carriers. The effective masses are extrapolated from the MP band structures using the BoltzTraP2 package [75,76] at room temperature and under low doping density. The position in the periodic table indicates the third constituent element of each PS.

find new materials (i) with low effective masses, required to achieve high μ, and (ii) with low defect densities and/or capture cross sections, required to achieve high τ. While we do not have exact answers to these questions at this stage, we will argue in the next three sections that there is significant scope for the discovery of new PSs with such desirable properties. The three main strategies we will outline are: Increasing the number of elements from ternary to quaternary compounds (Sec. 4.1), exploring P-rich compositions with P/S ≥ 1 (Sec. 4.2), and exploiting the chemical versatility of phosphorus (Sec. 4.3).

4.1 Increasing the number of elements

Unlike most elements, phosphorus can take a wide range of oxidation states from -3 to +5 in solid-state materials. PSs are an ideal material family to see these extreme oxidation states in action. We have already seen that compounds with P/S ≤ 1/3 prefer high positive oxidation states for phosphorus (+5, +4), whereas negative oxidation states (-1,-2,-3) are favored in compounds with P/S ≥ 1. Since phosphorus can easily form bonds with other P atoms in the solid state,[34,77] all other intermediate oxidation states are in principle possible. The availability of such a wide range of oxidation states indicates that there should be many combinations of elemental compositions that satisfy the requirement of charge neutrality. This translates into a large number of hypothetical PS materials that are chemically plausible and not intrinsically metallic.

To verify this hypothesis, we estimate the number of hypothetical charge-neutral PS compositions with the SMACT package [78]. For ternary PSs, the result is 1,737 distinct compositions assuming $M_aP_bS_c$ formulas including metals up to Bi and stoichiometric coefficients a,b,c between 0 and 10. For comparison, the number of charge-neutral ternary oxysulfides ($M_aO_bS_c$) is only 228 using the same rules. For quaternary PSs, the number of distinct charge-neutral composition is 202,829, assuming $M1_aM2_bP_cS_d$ formulas with stoichiometric coefficients up to 10. Again, the number of oxysulfides is significantly lower (31,499).

Although the charge neutrality filter does not guarantee thermodynamic stability, these numbers give an idea of the enormous size of the quaternary PS chemical space, even when compared to other quaternary spaces that do not contain elements with the same versatility as phosphorus. Besides the advantage in size, what are the prospects of finding high quality semiconductors among quaternary PSs? An encouraging trend is that the number of already-known stable quaternary PSs exceeds the number of corresponding ternaries (Figure 1). Hence, quaternary PSs should not have intrinsic problems with thermodynamic stability. Other promising features of the existing quaternary compounds are a higher fraction of materials with 3D structural dimensionality with respect to ternaries (Figure 3), and a higher fraction of materials with a P/S = 1/4 ratio (Figure 1), which typically have lower effective masses (Figure 4) than the P/S = 1/3 case.

Another question one may ask is: Can quaternary systems contain semiconductors with improved properties with respect to the ternaries? As an instructive example, let us consider the case of KAg_2PS_4 (mp-12532). In terms of composition, this compound only differs from Ag_3PS_4 (mp-12459) by the replacement of one Ag atom per formula unit by a K atom. Although the structures of the two materials are different, they are 3D in both cases. The band gap is predicted to increase from Ag_3PS_4 to KAg_2PS_4 (1.0 to 1.2 eV at the PBE level, 1.8 to 2.1 eV with HSE correction). Even though effective masses often tend to increase with increasing band gaps, [79] the direction-averaged hole effective mass of KAg_2PS_4 actually decreases by 0.48 m_0, while the electron effective mass remains approximately constant. The resulting effective masses in KAg_2PS_4 (0.25 m_0 for electrons, 0.78 m_0 for holes) are typical of high-quality optoelectronic semiconductors. This interesting trend might be explained in very qualitative terms by the inductive effect, [80] in which the presence of an electropositive cation (here, K^+) increases the covalency of the remaining bonds (here, Ag-S), and therefore the dispersion of the bands.

Although the band gap of KAg_2PS_4 is indirect (thus α might be low), this example demonstrates that the properties of quaternary PSs can be superior to the weighted average of the properties of their ternary constituents. Thus, we expect that optimal combinations of properties (high α, μ, and τ) should be accessible in quaternary PSs with an appropriate combination of elements.

4.2 Increasing the phosphorus content

We have seen that the majority of the known PSs are polyanionic thiophosphates with low P/S ratios (1/3 and below). Although a combination of visible band gaps and low effective masses can be found in some cases (Fig. 2 and Fig. 4), many thiophosphates exhibit relatively flat bands and high effective masses. Disperse bands and low effective masses seem to be more common in PSs with higher phosphorus content and with separate P and S anions, rather than polyanions. For example, a significant fraction of the known compounds with P/S = 1 have low effective masses (Fig.4). While this is a promising trend, three questions remain open for this class of PSs. 1) Are low effective masses common simply because compounds with P/S = 1 tend to have narrow band gaps? 2) Are compounds with P/S = 1 only thermodynamically stable when the metal belongs to either the d-block or the f-block? 3) Are there really so few quaternary compounds with P/S = 1 as Fig. 1b seems to suggest?

Moving to even P-richer compositions, all the currently known PSs with P/S = 2 (Ca_4P_2S, Sr_4P_2S, and Ba_4P_2S)[35] have a favorable combination of direct band gaps in the visible and low effective masses. The only compound we could find

with P/S = 3 is Zr_2P_3S (mp-1215423). This PS is only slightly metastable (18 meV above the convex hull) and is predicted to be a semimetal at the PBE level. Due to the systematic band gap underestimation of the PBE functional, Zr_2P_3S might as well be a semiconductor. It is also plausible that other ternary and quaternary compounds with P/S = 3 may exist.

In Fig. 5, we show some of the structural motifs seen in PS compounds with P/S ≥ 1 and independent P and S anions. They contrast with the polyanionic motifs shown in Fig. 1c for materials with lower P/S ratios. In some of the materials shown in Fig. 5 (Y_2PS, Ca_4P_2S) the coordination environments of P and S are nearly identical, which may promote disorder in the anion sublattice under certain experimental conditions. This can be a beneficial feature, because control over the order parameter in a semiconductor can be exploited to fine-tune its properties.[81] Other materials shown in Fig. 5 (YPS and Zr_2P_3S) have rather different coordination environments for P and S, so less prominent disorder effects are expected. Substantial P-S disorder also seems unlikely in thiophosphates because S and P are in significantly different chemical environments with very different oxidation states and ionic radii.

From the analysis in this section, we argue that research on P-rich phosphosulfides would be of particular interest, both for fundamental materials discovery and for optoelectronic energy conversion applications.

4.3 Exploiting the chemical versatility of phosphorus to engineer defect tolerance

Our analysis so far has focused on where to find PSs with low effective masses and direct band gaps in the visible. These features are correlated with high μ and high α in an appropriate photon energy range. However, we have not touched upon the third desirable feature mentioned in the Introduction, i.e., a high carrier lifetime τ. Compared to the case of α and μ, it is much more difficult to find simple properties available in materials databases that can be correlated to τ. The carrier lifetime is inversely related to the product of the concentration and capture cross section of crystal defects that are active as Shockley-Read-Hall recombination centers. In addition, the closer a defect state is to mid-gap, the higher the Shockley-Read-Hall recombination rate will tend to be at constant τ.[82] For most compound semiconductors, the dominant defects are not extrinsic impurities, but rather native defects that are thermodynamically favored. Developing general design rules for semiconductors with high τ and low recombination rates ("defect-tolerant") has proved elusive. Nevertheless, there is some consensus that the nature of the electronic states at the band edges plays an important role.[83–85] Relevant factors include the constituent orbitals, their hybridization, and whether they form bonding or antibonding states.

In this sense, the chemical versatility of PSs gives a design handle that is not available in most other material classes. To see how, we recall our conclusion (Sec. 3.3, Sec. 4.1, Sec. 4.2) that some semiconductors with high α and high μ are likely to be found among PSs with different P/S ratios and oxidation states. This implies that the phosphorus states can be "moved around" between the valence and the conduction band by changing the material, while still keeping a high α and high μ.

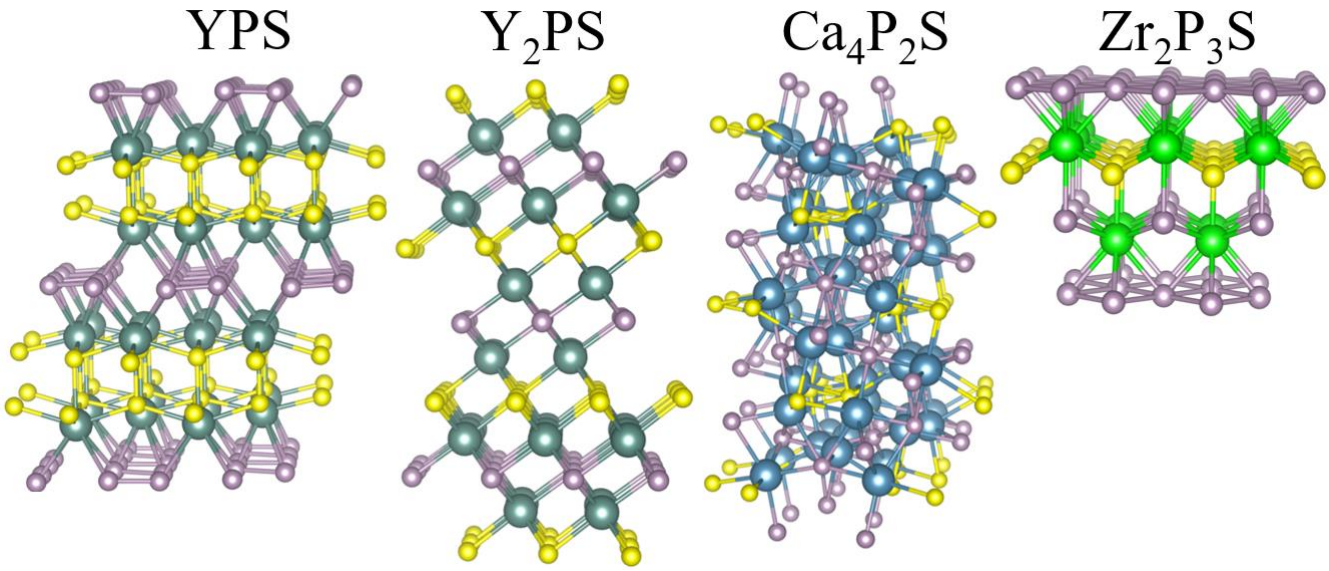

Figure 5. Some structural motifs seen in PSs with high P/S ratios and without P-S polyanions. The structures of PSs YPS (mp-1191026), Y_2PS (mp-1216056), Ca_4P_2S [35] and Zr_2P_3S (mp-1215423) are represented as a ball and stick model and *visualized with VESTA [32] Phosphorus is always displayed in purple, sulfur in yellow and the respective metal in the third colour. This figure is intended to complement Fig. 1 by including materials with separate P and S anions.*

Because the differences in P oxidation states in PSs are so large, we also expect large variations in hybridization and bonding types. It seems probable that some of these materials will be significantly more defect-tolerant than others, although it is impossible to determine which ones simply based on chemical intuition.

An exemplary case is the comparison of Ag_3PS_4 and Ba_4P_2S (Fig. 6). From a chemical standpoint, these two materials are completely different. Ag_3PS_4 is a 3D thiophosphate featuring the common $[PS_4]^{-3}$ tetrahedral polyanion, no metal-phosphorus bonds, and P in the +5 oxidation state. P states give an appreciable contribution to the conduction band minimum (CBM), which is predominantly of Ag(s) character. The valence band maximum (VBM) consists of hybridized Ag(d)-S(p) orbitals and contains no meaningful contributions from P states. Ba_4P_2S is a 3D PS with independent P^{3-} and S^{2-} anions and no other bonds than metal-P and metal-S bonds. Opposite to the case of Ag_3PS_4, the VBM of Ba_4P_2S is dominated by P(p) states as in III-V semiconductors. On the other hand, the CBM in Ba_4P_2S is mainly composed of Ba(d) states without substantial contributions from P orbitals. Although sulfur states give important contribution to both band edges in Ag_3PS_4, they are virtually absent in Ba_4P_2S.

Despite all these differences, we recognize similar desirable features in the band structures (visualized with the GPAW code[86]) of Ag_3PS_4 and Ba_4P_2S (Fig. 6). Band gaps are direct and lie in the visible (after applying the HSE correction), and both the CBM and the VBM have high band dispersion. Thus, both materials have significant potential for high α and high μ. Since the chemical origin of the band edges is completely different in the two materials, tuning the P/S ratio (or equivalently, the oxidation state of P) is a design knob unique to PSs. As the character of the band edges can be tuned

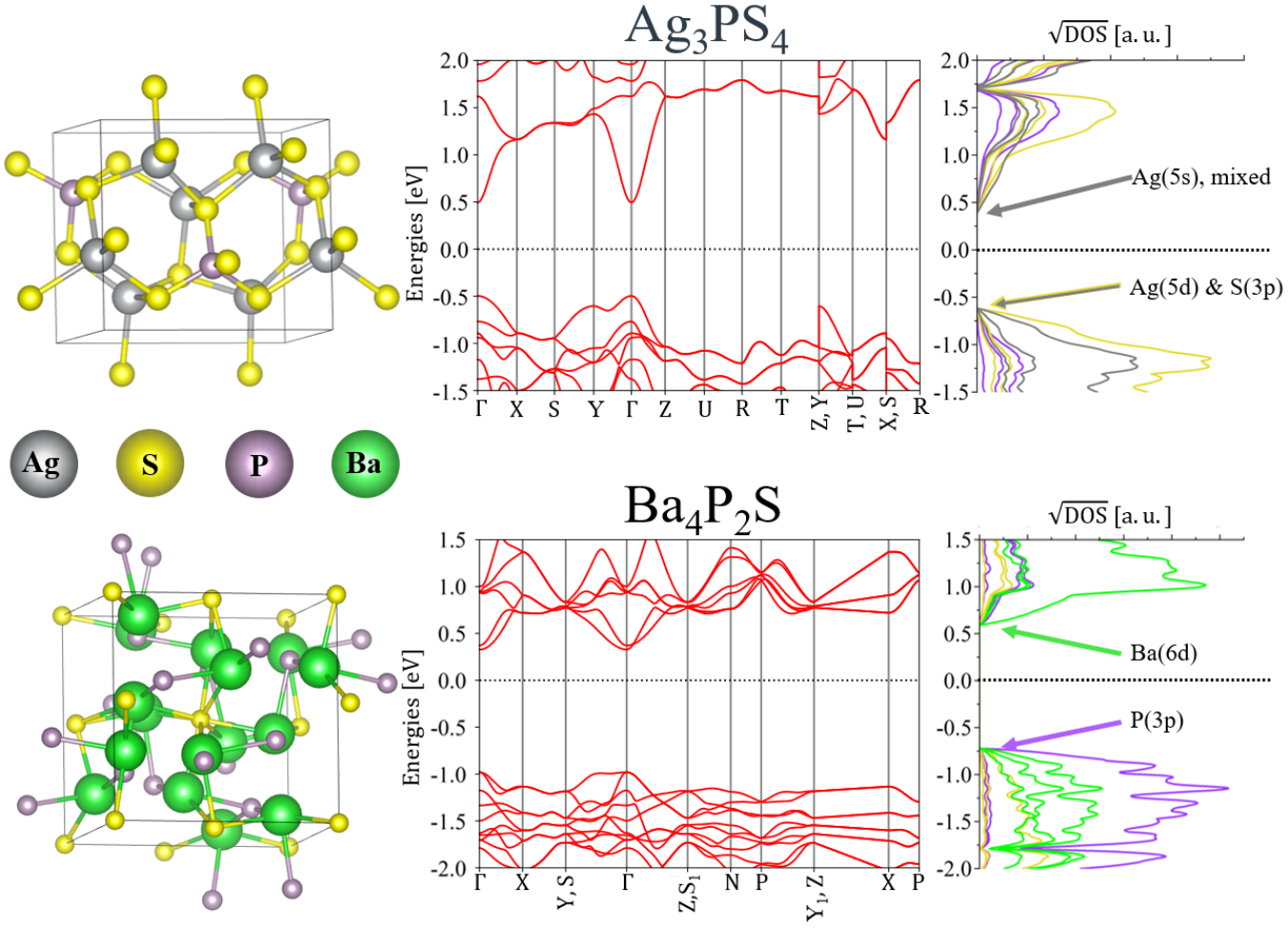

Figure 6. Comparison of Ag_3PS_4 (mp-12459) and Ba_4P_2S [35] as a demonstration of the unique chemical versatility of PSs. The crystal structure, electronic band structure, and orbital-resolved electronic density of states (DOS) are shown for Ag_3PS_4 (top row) and Ba_4P_2S (bottom row). Most of this information is already available elsewhere. [14,35] For the sake of consistency, we have recalculated the band structures and DOS at the PBE level using the GPAW code. [86] Even though the character of the band edges is entirely different in the two materials (see DOS), the resulting band structures have similar features (direct band gaps, disperse bands). The same color code is used for atoms and for electronic states. Silver is displayed in grey, sulfur in yellow, phosphorus in purple and barium in green.

while preserving an optimal band structure, we believe it may be possible to "screen for defect tolerance" by a combined computational and experimental approach, with the ultimate goal of achieving a high τ.

5. Prospects for experimental discovery and development of phosphosulfide semiconductors

We have argued that the space of unexplored PSs is vast, with considerable potential for finding high-quality semiconductors. Computational screening methods based on high-throughput DFT are a useful tool to search for materials with the desired properties in large chemical spaces.[87,88] However, some of the key properties that are linked to high PV performance (most notably τ) are prohibitively expensive to calculate for more than a handful of materials.[89] Additionally, many physical effects that are likely to affect the experimental τ (defect clusters, entropic effects, grain boundaries etc.) have to be neglected to make the problem computationally treatable. Finally, it is challenging to predict the properties of hypothetical materials with unknown crystal structures, because both composition and structure are required in first-principles calculations as input. Many hypothetical PSs with P/S > 1 and many hypothetical quaternary PSs have unknown crystal structures. Thus, we argue that high-throughput experiments [90–92] are necessary to rapidly explore the synthesizability and properties of known and unknown PS semiconductors.

5.1 Potential synthesis methods

Let us consider the synthesis methods reported for PSs so far. Are any of them appropriate for high-throughput studies of optoelectronic materials? Most authors have employed classic high-temperature solid-state reactions and chemical vapor transport of bulk PS powders and crystals.[17,21,31,48,93] These approaches are low-throughput, as the timeframe for a synthesis run is often in the range of weeks, due to the slow solid-state diffusion process in bulk materials.

Many known PS crystals with 2D dimensionality have been exfoliated to produce one- or few-atom-thin 2D PSs. However, neither the crystal growth nor the exfoliation process are high-throughput, and this method cannot be used for materials with 3D dimensionality. Very recently, Zhou et al. reported a versatile chemical vapor deposition (CVD) method enabling the growth of 8 atomically-thin ternary thiophosphates, as well as 5 quaternary thiophosphate solid solutions.[72] The precursors for sulfur and phosphorus were the elemental solids. Metal chloride powders were used as metal precursors. The vapor composition was simply the evaporated precursors in an Ar/H_2 carrier gas. While this method was designed for atomically thin 2D materials, it may be possible to extend it to grow thicker films of any dimensionality. Some high-throughput capabilities might be engineered in a CVD setup by exploiting temperature gradients at the substrate and in the precursors.

Several papers have reported synthesis of PSs of various dimensionalities as nanoparticles or other nanostructured forms.[26,30,61,94–96] Although nanoparticle synthesis is amenable to high-throughput combinatorial experiments,[90] material properties may be affected by size effects. Further, measurements of various electrical and optical properties require aggregation of nanoparticles into larger units (typically thin films). In these cases, problems with insufficient nanoparticle coalescence and film compactness can affect the results.

Interestingly, thin films are among the least commonly investigated material forms for PSs. To the best of our knowledge, thin-film synthesis has only been reported for six of the 258 experimentally synthesized PSs present in the ICDS database (Fig. 1). All of them are thiophosphates: $BiPS_4$ [26,59], Cu_3PS_4 [30,61], $Sn_2P_2S_6$ [45], Li_3PS_4 [97], Na_3PS_4 [98], and members of the Li-Ge-P-S system [99]. Relevant optoelectronic characterization was conducted for $BiPS_4$ and Cu_3PS_4, but these films consisted of spin- or drop-cast nanoparticles and may not be fully representative of fully coalesced polycrystalline films. The other films were grown by standard deposition techniques (thermal evaporation or pulsed laser deposition) but they were not optoelectronically characterized.

Despite their very limited presence in literature, we believe thin-film samples are the most convenient option for high-throughput discovery and development of PS semiconductors for optoelectronics. One of the main reasons is that it is relatively straightforward to engineer compositional and/or temperature gradients along two independent directions of the substrate in a single growth run using physical vapor deposition methods. These gradients typically result in material property variations across the substrate, which can be quickly measured by characterization instruments equipped with automated stages. Thus, it becomes possible to collect property-versus-composition or property-versus-process-parameter combinatorial libraries with a high throughput across ternary and quaternary systems alike. This combinatorial approach to materials research for optoelectronic semiconductors has already been applied to both thin-film sulfides and thin-film phosphides.[33,100–102]

In addition to their compatibility with high-throughput methods, thin films grown from controlled deposition sources are usually compact and have smooth interfaces. These features are ideal for optical and electrical measurements. Finally, standard thin-film thicknesses between tens of nm and a few μm are in the optimal range for most PV/PEC absorbers and LED emitters with reasonable properties. In fact, the large majority of solar cell technologies with meaningful efficiencies is based on thin-film PV absorbers,[13,74] with silicon being a notable exception due to its unusually low light

absorption coefficient. Hence, basic materials research on thin-film samples can immediately be translated into device prototypes.

While this article has so far focused on the discovery of new PS compounds, thin-film combinatorial methods are also ideal for studying PS solid solutions, structural disorder, doping by impurities, and the effects of non-stoichiometry. In fact, some quaternary PSs may be more stable in the form of pseudo-binary solid solutions, rather than as unique compounds. The GaP-ZnS solution is a well-documented example.[95,103,104] Recent CVD work on atomically-thin PSs also demonstrated growth of 5 quaternary solid solutions.[72] Ternary PSs are unlikely to form solid solutions in theory, because S and P have a different number of valence electrons, so charge neutrality is difficult to enforce with a single metallic element. Nevertheless, Li- and Cu-based PS solid solutions have been reported in certain composition ranges.[52,105] Sulfur is also known to be an effective dopant in GaP.[106]

5.2 Our strategy for rapid exploration of phosphosulfide semiconductor thin films

Our vision for high-throughput experimental exploration of PS thin films is summarized by the cartoons in Fig. 6. The full synthesis suite consists of three glove box-integrated tools with access to reactive sources of P and S (Fig. 6a). The tools are a reactive sputter system, a reactive rapid thermal annealing furnace (RRTP), and a simple thermal evaporator. Among them, the main deposition technique is combinatorial reactive sputtering (Fig. 6b), an established method to create combinatorial libraries by taking advantage of elemental composition- and growth temperature gradients across the substrate.[33,34,90,91,100,101,107,108] Reactive gaseous sources of S and P are rather uncommon in sputter deposition systems. Nevertheless, the few examples available in the literature have demonstrated high versatility and high material quality.[33,34,34,100,107–111]

For a generic quaternary PS system M1-M2-P-S (where M1 and M2 are two different metals), a desirable outcome of sputter deposition of PSs is a combinatorial library with a gradient in the M1/M2 ratio in one direction, and in the P/S ratio in the perpendicular direction (Fig. 6c). A M1/M2 gradient is straightforward to obtain by appropriate orientation of the M1 and M2 targets (Fig. 6b). Conversely, the P/S ratio gradient is difficult to achieve if both the P and the S sources are non-directional, as for the case of H_2S and PH_3 gases. A possible solution is to employ compound targets (a metal sulfide and a metal phosphide) rather than metallic targets. However, many of such targets are not commercially available, they have a high cost, a low deposition rate, and the target stoichiometry limits the range of compositions achievable in the final film. In our opinion, a more versatile solution to obtain P/S composition gradients is to employ a directional source for either sulfur or phosphorus, or both. Shown in Fig. 6(b) is the combination of a non-directional PH_3 source for P, and a directional evaporation source for S. Due to the very high vapor pressure of S_8 (the standard solid-state form of sulfur) and its relatively low reactivity at low temperatures, S_8 is first evaporated at a low temperature in an effusion cell. Then, it is cracked into smaller, more reactive molecules in a separate high-temperature zone of the source. By appropriate orientation of the sulfur source, the result shown in Fig. 6c is expected, which gives rise to the desired orthogonal gradients in composition.

There are two remaining potential problems with a PS film synthesis approach exclusively based on reactive sputtering. The first is linked to the volatility of S and P, even when incorporated in solid-state compounds. For many metal sulfides and phosphides, heating in a non-reactive atmosphere leads to decomposition reactions, typically resulting in preferential loss of S in sulfide films [112] and P in phosphide films.[34,111] Since temperatures significantly above room temperature are required to crystallize most inorganic materials, the decomposition temperature may be lower than the crystallization temperature for a wide range of targeted PS compounds. The solution to this problem is to ensure high partial pressures of S and P during high-temperature crystallization. Since these species are the gaseous products of decomposition reactions, their intentional addition to the gas mix pushes the decomposition reaction towards the left (i.e., towards the desired solid PS compound) due to Le Chatelier's principle. While relatively high concentrations of S and P in the gas phase could potentially be enforced in the sputter system described above, their partial pressures would still be rather low, because the total pressure in a sputter deposition process is limited to the 10^{-6}–10^{-5} bar range.[113]

Reactive annealing of the sputter-deposited combinatorial libraries in a separate RRTP unit with access to gaseous PH_3 and H_2S sources and an accessible total pressure up to 1 bar can solve this problem. Another advantage of including an RRTP setup is that it is technically much easier to reach temperatures in excess of 1000 °C and avoid corrosion in an RTP furnace than in a sputter system. In fact, an ex-situ annealing step in a S-containing atmosphere is common practice in sulfide thin film synthesis [114–118] as it can ensure film crystallization without the loss of sulfur. In many labs, transferring a thin film from deposition equipment to reactive annealing equipment requires exposure to ambient air. This limits the applicability of the two-step film growth process (deposition + annealing) to materials that do not react with oxygen or moisture when they are not crystallized or not fully sulfurized/phosphorized. Sacrificial capping layers can be deposited on top of air-sensitive films to slow down their reaction with air,[115] but this adds complication to the process, and at least a small fraction of the capping layer is likely to be incorporated into the final film and may affect its

electronic properties. Transfer of thin-film samples between the deposition and the annealing systems in a glove box under an inert atmosphere (Fig. 6a) can solve these issues.

The second potential problem with PS thin-film synthesis is dealing with M1-M2-P-S material systems where either M1 or M2 is a volatile metal. Such "problematic" metals are Group 1 (alkalis), Group 2 (alkaline earths), and Group 12 elements. Since volatile metals tend to sublime in vacuum at very low temperatures, they are difficult to sputter in a controlled manner and can cause contamination problems that are in some cases irreparable. To address this problem, we propose the inclusion of a very simple thermal evaporator with replaceable parts in the deposition suite (Fig. 6a). In this separate chamber, Group 2 and Group 12 elements (constituting, say, M1 in the M1-M2-P-S system of interest) can be deposited from metal sources, while the substrate is not intentionally heated. In a thermal evaporator, even Group 1 elements can be evaporated as pure metals by using alkali metal dispensers as sources [119]. The volatile M1 can be evaporated before or after sputter deposition of a M2-P-S combinatorial library, and the resulting M1/M2-P-S film stack can be reactively annealed in the RRTP to aim for crystallization of the M1-M2-P-S material of interest. Due to the typically high solid-state diffusion coefficients in volatile metals, no significant kinetic barriers are expected for the diffusion of the M1 layer into the M2-P-S matrix. Glove-box

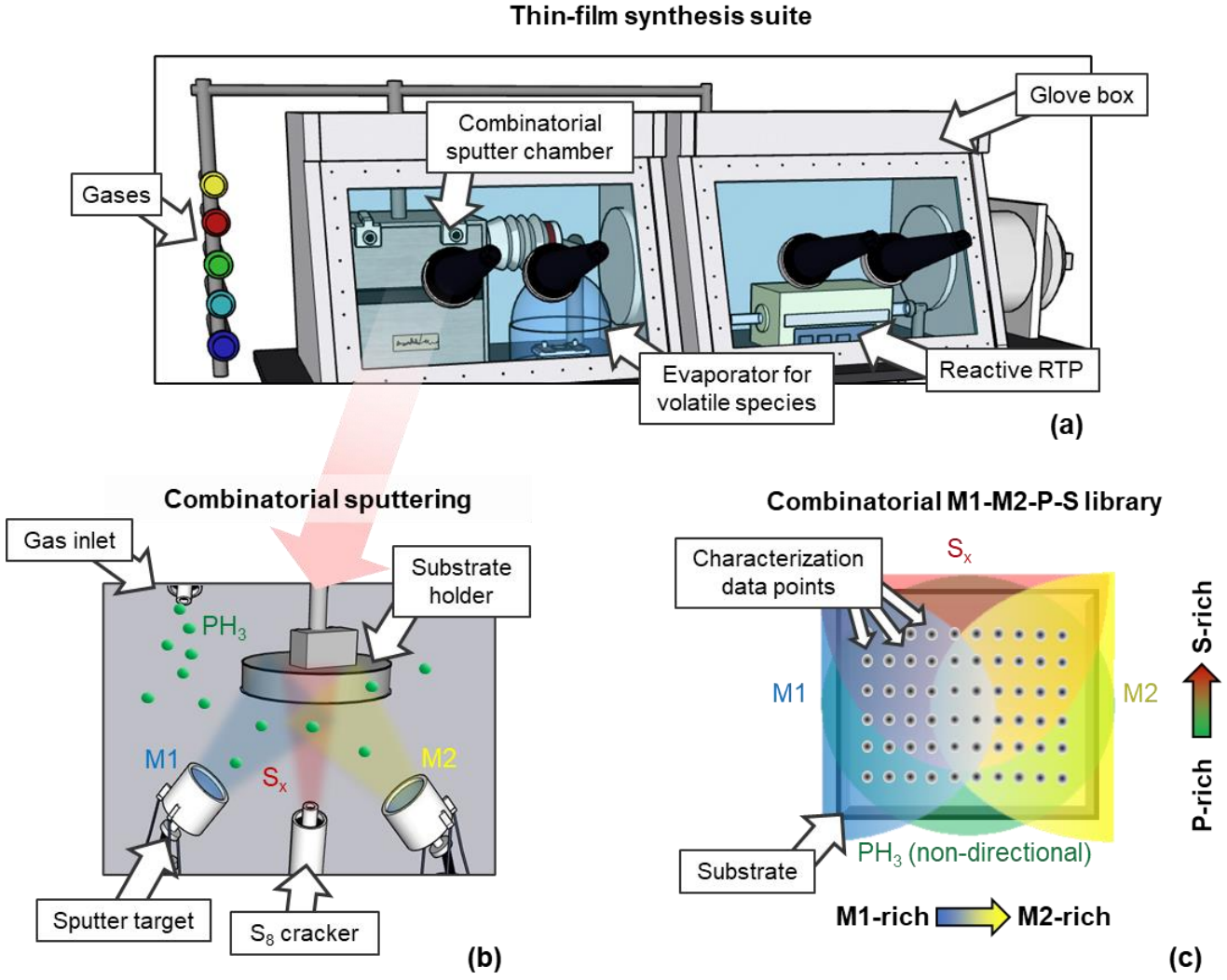

*Figure 7: Cartoon of a PS-dedicated thin-film synthesis suite for high-throughput development of PS semiconductors. **a)**: Overview of the glove-box-integrated system with the three individual setups described in the main article. **a)**: Overview of the glove-box-integrated system with the three individual setups described in the main article. **b)**: Scheme of the combinatorial reactive sputter process involving two metal targets (M1 and M2), a directional S source (the S_8 cracker), and a diffuse P source (diluted PH_3 gas). **c)**: Example of a combinatorial thin-film material library on a substrate, as expected from the combinatorial sputter deposition process. The arrows indicate gradients in elemental composition due to the directionality of the sources. The dots indicate potential measurement points for high-throughput characterization of material properties as a function of composition.*

integration is key for handling and transfer of the air-sensitive Group 1 and Group 2 metal thin films.

A thin-film deposition suite similar to the one described in this section has been designed and is currently being installed in our laboratory. It is our hope that it will allow rapid combinatorial exploration of (almost) any ternary and quaternary PS system with any molar ratio between the desired metals, and with a very wide range of P/S ratios. Clearly, there should be effective safety measures in place before working with such a setup. Among them, the potential release of PH_3 and H_2S gases should be prevented, reaction products should be neutralized, and materials of unknown toxicity and reactivity should be appropriately handled.

6. Conclusion

We reviewed trends in composition, structure, and optoelectronic properties of inorganic phosphosulfides, aided by the existing literature and the Materials Project database. Based on this analysis, we assessed their potential as semiconductors for optoelectronic energy conversion applications. We believe that phosphosulfides deserve much closer research attention, as this material family likely contains semiconductors with strong light absorption and favorable charge transport and recombination properties. The main arguments leading to this recommendation are the following:

1) Among the known phosphosulfides, the majority are semiconductors with band gaps in the visible and three-dimensional structural networks, indicating their potential to absorb relevant fractions of the solar spectrum and to ensure good electronic transport in all directions.
2) Direct-gap, low-effective-mass semiconductors are already known in ternary phosphosulfide systems (e.g., Ag_3PS_4, Ba_4P_2S), even though 3D structural networks in PSs do not always translate to low effective masses.
3) The high chemical versatility of phosphorus in phosphosulfides implies that direct-gap, low-effective-mass semiconductors can be generated by completely different combinations of frontier orbitals. Ag_3PS_4 and Ba_4P_2S illustrate this concept. This is a unique design handle for phosphosulfides, and it could be exploited to engineer defect tolerance by engineering the orbital character of the bands.
4) Phosphosulfides are a vast material space, because of the wide allowed range of phosphorus oxidation states. We estimate that the number of chemically plausible phosphosulfides exceeds the corresponding number of oxysulfides by almost an order of magnitude.
5) Phosphorus-rich phosphosulfides (i.e., those with P/S > 1) have never been synthesized. Nevertheless, the few ones that have been computationally studied appear to be thermodynamically stable and with optimal optoelectronic features.
6) Quaternary phosphosulfides are often thermodynamically stable, and there are concrete examples of quaternaries with improved optoelectronic properties with respect to their ternary constituents. KAg_2PS_4 is an illustrative case.

We recommend the utilization of high-throughput experimental methods to screen a larger range of the PSs in thin-film form and exploit synergies with the modern arsenal of computational materials science, including high-throughput DFT and machine learning. In concrete terms, we propose a custom suite of thin-film growth setups centered around reactive combinatorial sputter deposition, including options for reactive annealing and incorporation of volatile metals by thermal evaporation.

Acknowledgements

We acknowledge Javier Sanz Rodrigo and Maarten Goesten for useful discussions. We are grateful to Bettina Aagaard Vester for drawing the original version of Figure 7. This work was supported in part by a research grant (42140) from VILLUM FONDEN and co-funded by the European Union (ERC, IDOL, 101040153). Views and opinions expressed are, however, those of the author only and do not necessarily reflect those of the European Union or the European Research Council. Neither the European Union nor the granting authority can be held responsible for them.

References

[1] Kaienburg P, Krückemeier L, Lübke D, Nelson J, Rau U and Kirchartz T 2020 How solar cell efficiency is governed by the α μ τ product *Phys. Rev. Res.* **2** 023109

[2] Sivula K and van de Krol R 2016 Semiconducting materials for photoelectrochemical energy conversion *Nat. Rev. Mater.* **1** 15010

[3] Würfel P and Würfel U 2010 *Physics of solar cells* (Wenheim: Wiley-VCH Verlag GmbH)

[4] Ganose A M, Scanlon D O, Walsh A and Hoye R L Z 2022 The defect challenge of wide-bandgap semiconductors for photovoltaics and beyond *Nat. Commun.* **13** 4715

[5] Pamplin B R 1964 A systematic method of deriving new semiconducting compounds by structural analogy *J. Phys. Chem. Solids* **25** 675–84

[6] Wang J, Chen H, Wei S-H and Yin W-J 2019 Materials Design of Solar Cell Absorbers Beyond Perovskites and Conventional Semiconductors via

Combining Tetrahedral and Octahedral Coordination *Adv. Mater.* **31** 1806593

[7] Choi J W, Shin B, Gorai P, Hoye R L Z and Palgrave R 2022 Emerging Earth-Abundant Solar Absorbers *ACS Energy Lett.* **7** 1553–7

[8] Vegard L 1921 Die Konstitution der Mischkristalle und die Raumfüllung der Atome *Z. Für Phys.* **5** 17–26

[9] Gschneidner K A Jr and Vineyard G H 2004 Departures from Vegard's Law *J. Appl. Phys.* **33** 3444–50

[10] Kageyama H, Hayashi K, Maeda K, Attfield J P, Hiroi Z, Rondinelli J M and Poeppelmeier K R 2018 Expanding frontiers in materials chemistry and physics with multiple anions *Nat. Commun.* **9** 772

[11] Miyoshi A and Maeda K 2021 Recent Progress in Mixed-Anion Materials for Solar Fuel Production *Sol. RRL* **5** 2000521

[12] Crovetto A, Hajijafarassar A, Hansen O, Seger B, Chorkendorff I and Vesborg P C K 2020 Parallel Evaluation of the BiI_3 , BiOI, and Ag_3BiI_6 Layered Photoabsorbers *Chem. Mater.* **32** 3385–95

[13] Zakutayev A, Major J D, Hao X, Walsh A, Tang J, Todorov T K, Wong L H and Saucedo E 2021 Emerging inorganic solar cell efficiency tables (version 2) *J. Phys. Energy* **3** 032003

[14] Jain A, Ong S P, Hautier G, Chen W, Richards W D, Dacek S, Cholia S, Gunter D, Skinner D, Ceder G and Persson K A 2013 Commentary: The Materials Project: A materials genome approach to accelerating materials innovation *APL Mater.* **1** 011002

[15] Zagorac D, Müller H, Ruehl S, Zagorac J and Rehme S 2019 Recent developments in the Inorganic Crystal Structure Database: theoretical crystal structure data and related features *J. Appl. Crystallogr.* **52** 918–25

[16] Susner M A, Chyasnavichyus M, McGuire M A, Ganesh P and Maksymovych P 2017 Metal Thio- and Selenophosphates as Multifunctional van der Waals Layered Materials *Adv. Mater.* **29** 1602852

[17] Chen Z-X, Liu W and Guo S-P 2023 A review of structures and physical properties of rare earth chalcophosphates *Coord. Chem. Rev.* **474** 214870

[18] Evain M, Brec R and Whangbo M-H 1987 Structural and electronic properties of transition metal thiophosphates *J. Solid State Chem.* **71** 244–62

[19] Wu Y and Bensch W 2010 Structural diversity of rare earth and transition metal thiophosphates *CrystEngComm* **12** 1003–15

[20] Yang Y, Song M, Wu X and Wu K 2021 A review of the structural diversity of $[P_xS_y]^{n-}$motifs and their potential application prospects in metal thiophosphates *J. Phys. Appl. Phys.* **54** 463002

[21] Samal R, Sanyal G, Chakraborty B and Rout C S 2021 Two-dimensional transition metal phosphorous trichalcogenides (MPX_3): a review on emerging trends, current state and future perspectives *J. Mater. Chem. A*

[22] Liu J, Li X, Xu Y, Ge Y, Wang Y, Zhang F, Wang Y, Fang Y, Yang F, Wang C, Song Y, Xu S, Fan D and Zhang H 2019 $NiPS_3$ nanoflakes: a nonlinear optical material for ultrafast photonics *Nanoscale* **11** 14383–91

[23] Ji B, Sarkar A, Wu K, Swindle A and Wang J 2022 $A_2P_2S_6$ (A = Ba and Pb): a good platform to study the polymorph effect and lone pair effect to form an acentric structure *Dalton Trans.* **51** 4522–31

[24] Peng W, Li J, Shen K, Zheng L, Tang H, Gong Y, Zhou J, Chen N, Zhao S, Chen M, Gao F and Gou H 2020 Iron-regulated NiPS for enhanced oxygen evolution efficiency *J. Mater. Chem. A* **8** 23580–9

[25] Roy P K, Antonatos N, Li T, Jing Y, Luxa J, Azadmanjiri J, Marvan P, Heine T and Sofer Z 2023 2D Few-Layered PdPS: Toward High-Efficient Self-Powered Broadband Photodetector and Sensors *ACS Appl. Mater. Interfaces* **15** 1859–70

[26] Shaddad M N, Arunachalam P, Hezam M, BinSaeedan N M, Gimenez S, Bisquert J and Al-Mayouf A M 2023 Facile fabrication of heterostructured $BiPS_4$-Bi_2S_3-$BiVO_4$ photoanode for enhanced stability and photoelectrochemical water splitting performance *J. Catal.* **418** 51–63

[27] Song B-J, Ma Z, Li B, Wu X-T, Lin H and Zhu Q-L 2021 Structural Modulation from Cu_3PS_4 to $Cu_5Zn_{0.5}P_2S_8$: Single-Site Aliovalent-Substitution-Driven Second-Harmonic-Generation Enhancement *Inorg. Chem.* **60** 4357–61

[28] Sultana U K and O'Mullane A P 2018 Electrochemical Formation of Amorphous Molybdenum Phosphosulfide for Enabling the Hydrogen Evolution Reaction in Alkaline and Acidic Media *ACS Appl. Energy Mater.* **1** 2849–58

[29] Wang M, Saad A, Li X, Peng T, Zhang Q-T, Kumar M and Zhao W 2021 Solid-state synthesis of single-

phase nickel monophosphosulfide for the oxygen evolution reaction *Dalton Trans.* **50** 12870–8

[30] Yin X, McClary S A, Song Z, Zhao D, Graeser B, Wang C, Shrestha N, Wang X, Chen C, Li C, Subedi K K, Ellingson R J, Tang W, Agrawal R and Yan Y 2019 A Cu_3PS_4 nanoparticle hole selective layer for efficient inverted perovskite solar cells *J. Mater. Chem. A* **7** 4604–10

[31] Zhu M, Kou H, Wang K, Wu H, Ding D, Zhou G and Ding S 2020 Promising functional two-dimensional lamellar metal thiophosphates: synthesis strategies, properties and applications *Mater. Horiz.*

[32] Momma K and Izumi F 2011 VESTA 3 for three-dimensional visualization of crystal, volumetric and morphology data *J. Appl. Crystallogr.* **44** 1272–6

[33] Schnepf R R, Crovetto A, Gorai P, Park A, Holtz M, Heinselman K N, Bauers S R, Tellekamp M B, Zakutayev A, Greenaway A L, Toberer E S and Tamboli A C 2022 Reactive phosphine combinatorial co-sputtering of cation disordered $ZnGeP_2$ films *J. Mater. Chem. C* **10** 870–9

[34] Crovetto A, Kojda D, Yi F, Heinselman K N, LaVan D A, Habicht K, Unold T and Zakutayev A 2022 Crystallize It before It Diffuses: Kinetic Stabilization of Thin-Film Phosphorus-Rich Semiconductor CuP_2 *J. Am. Chem. Soc.* **144** 13334–43

[35] Amsler M, Ward L, Hegde V I, Goesten M G, Yi X and Wolverton C 2019 Ternary mixed-anion semiconductors with tunable band gaps from machine-learning and crystal structure prediction *Phys. Rev. Mater.* **3** 035404

[36] Kamaya N, Homma K, Yamakawa Y, Hirayama M, Kanno R, Yonemura M, Kamiyama T, Kato Y, Hama S, Kawamoto K and Mitsui A 2011 A lithium superionic conductor *Nat. Mater.* **10** 682–6

[37] Brehm J A, Neumayer S M, Tao L, O'Hara A, Chyasnavichus M, Susner M A, McGuire M A, Kalinin S V, Jesse S, Ganesh P, Pantelides S T, Maksymovych P and Balke N 2020 Tunable quadruple-well ferroelectric van der Waals crystals *Nat. Mater.* **19** 43–8

[38] Kang S, Kim K, Kim B H, Kim J, Sim K I, Lee J-U, Lee S, Park K, Yun S, Kim T, Nag A, Walters A, Garcia-Fernandez M, Li J, Chapon L, Zhou K-J, Son Y-W, Kim J H, Cheong H and Park J-G 2020 Coherent many-body exciton in van der Waals antiferromagnet $NiPS_3$ *Nature* **583** 785–9

[39] Park K H, Bai Q, Kim D H, Oh D Y, Zhu Y, Mo Y and Jung Y S 2018 Design Strategies, Practical Considerations, and New Solution Processes of Sulfide Solid Electrolytes for All-Solid-State Batteries *Adv. Energy Mater.* **8** 1800035

[40] Zhou W, Wu J, Liu W and Guo S-P 2023 Ag-based chalcogenides and derivatives as promising infrared nonlinear optical materials *Coord. Chem. Rev.* **477** 214950

[41] Ho S-F and Tuan H-Y 2023 Cu_3PS_4: a sulfur-rich metal phosphosulfide with superior ionic diffusion channel for high-performance potassium ion batteries/hybrid capacitors *Chem. Eng. J.* **452** 139199

[42] Tripathy D and Sampath S 2020 Understanding the high capacity contributions of Cu_3PS_4 towards lithium storage *J. Power Sources* **478** 229066

[43] Chen X, Ding X, Muheiyati H, Feng Z, Xu L, Ge W and Qian Y 2019 Hierarchical flower-like cobalt phosphosulfide derived from Prussian blue analogue as an efficient polysulfides adsorbent for long-life lithium-sulfur batteries *Nano Res.* **12** 1115–20

[44] Ng S-F, Lau M Y L and Ong W-J 2021 Lithium–Sulfur Battery Cathode Design: Tailoring Metal-Based Nanostructures for Robust Polysulfide Adsorption and Catalytic Conversion *Adv. Mater.* **33** 2008654

[45] Bogomolov A A, Solnyshkin A V, Kiselev D A, Raevskii I P, Shonov V Y and Sandzhiev D N 2008 Temperature behavior of the photovoltaic and pyroelectric responses of $Sn_2P_2S_6$ semiconductor ferroelectric films *J. Surf. Investig. X-Ray Synchrotron Neutron Tech.* **2** 496–501

[46] Liu F, You L, Seyler K L, Li X, Yu P, Lin J, Wang X, Zhou J, Wang H, He H, Pantelides S T, Zhou W, Sharma P, Xu X, Ajayan P M, Wang J and Liu Z 2016 Room-temperature ferroelectricity in $CuInP_2S_6$ ultrathin flakes *Nat. Commun.* **7** 12357

[47] Belianinov A, He Q, Dziaugys A, Maksymovych P, Eliseev E, Borisevich A, Morozovska A, Banys J, Vysochanskii Y and Kalinin S V 2015 $CuInP_2S_6$ Room Temperature Layered Ferroelectric *Nano Lett.* **15** 3808–14

[48] Rahman S, Torres J F, Khan A R and Lu Y 2021 Recent Developments in van der Waals Antiferromagnetic 2D Materials: Synthesis, Characterization, and Device Implementation *ACS Nano* acsnano.1c06864

[49] Brec R 1986 Review on structural and chemical properties of transition metal phosphorous trisulfides MPS_3 *Solid State Ion.* **22** 3–30

[50] Mayorga-Martinez C C, Sofer Z, Sedmidubský D, Huber Š, Eng A Y S and Pumera M 2017 Layered Metal Thiophosphite Materials: Magnetic, Electrochemical, and Electronic Properties *ACS Appl. Mater. Interfaces* **9** 12563–73

[51] Andreev A, Ivanova V, Kirilov K and Passage G 1994 Catalytic oxidation of sulfide ions over $NiPS_3$ *Appl. Catal. Gen.* **107** 189–99

[52] Zhang X, Kim D, Yan J and Lee L Y S 2021 Photocatalytic CO_2 Reduction Enabled by Interfacial S-Scheme Heterojunction between Ultrasmall Copper Phosphosulfide and g-C_3N_4 *ACS Appl. Mater. Interfaces* **13** 9762–70

[53] Roy P K, Marvan P, Mazánek V, Antonatos N, Bouša D, Kovalska E, Sedmidubský D and Sofer Z 2021 Self-Powered Broadband Photodetector and Sensor Based on Novel Few-Layered $Pd_3(PS_4)_2$ Nanosheets *ACS Appl. Mater. Interfaces* **13** 30806–17

[54] Feng J, Long C, Yao L-J, Hu C-L and Mao J-G 2022 α- and β-$Ag_4P_2S_7$: Two Semiconductors with Promising Photocatalytic Hydrogen Production Based on a Density Functional Theory Study *Inorg. Chem.* **61** 6711–4

[55] Wang S, Fan N, Zhou Z, Hu Y, Hui Q, Li Q, Xue J, Zhou Z, Feng Z, Yan Q, Weng Y, Tang R, Zheng F, Fan R, Xu B, Fang L and You L 2022 Self-Enhancing Photoelectrochemical Properties in van der Waals Ferroelectric $CuInP_2S_6$ by Photoassisted Acid Hydrolysis *ACS Appl. Mater. Interfaces* **14** 40126–35

[56] Barua M, Ayyub M M, Vishnoi P, Pramoda K and Rao C N R 2019 Photochemical HER activity of layered metal phospho-sulfides and -selenides *J. Mater. Chem. A* **7** 22500–6

[57] Liu T, Xiao W, Luo Z, Bi J, Zhang Y, Wang G, Wang D and Liu X 2022 Regulating on photocatalytic overall water splitting performance of gallium thiophosphate based on transition metal doping: A first-principles study *Mol. Catal.* **533** 112765

[58] Han D and Ebert H 2021 Identification of Potential Optoelectronic Applications for Metal Thiophosphates *ACS Appl. Mater. Interfaces* **13** 3836–44

[59] Tiwari D, Alibhai D, Cherns D and Fermin D J 2020 Crystal and Electronic Structure of Bismuth Thiophosphate, $BiPS_4$: An Earth-Abundant Solar Absorber *Chem. Mater.* **32** 1235–42

[60] Itthibenchapong V, Kokenyesi R S, Ritenour A J, Zakharov L N, Boettcher S W, Wager J F and Keszler D A 2013 Earth-abundant Cu-based chalcogenide semiconductors as photovoltaic absorbers *J Mater Chem C* **1** 657–62

[61] Sheets E J, Yang W-C, Balow R B, Wang Y, Walker B C, Stach E A and Agrawal R 2015 An in situ phosphorus source for the synthesis of Cu_3P and the subsequent conversion to Cu_3PS_4 nanoparticle clusters *J. Mater. Res.* **30** 3710–6

[62] Shen T, Zhang C, Qiu C and Deng H-X 2022 Origin of the discrepancy between the fundamental and optical gaps and native defects in two dimensional ultra-wide bandgap semiconductor: Gallium thiophosphate *Appl. Phys. Lett.* **120** 172108

[63] Brec R, Schleich D M, Ouvrard G, Louisy A and Rouxel J 1979 Physical properties of lithium intercalation compounds of the layered transition-metal chalcogenophosphites *Inorg. Chem.* **18** 1814–8

[64] Zhang X, Zhao X, Wu D, Jing Y and Zhou Z 2016 MnPSe3 Monolayer: A Promising 2D Visible-Light Photohydrolytic Catalyst with High Carrier Mobility *Adv. Sci.* **3** 1600062

[65] Li Y, Fu J, Mao X, Chen C, Liu H, Gong M and Zeng H 2021 Enhanced bulk photovoltaic effect in two-dimensional ferroelectric $CuInP_2S_6$ *Nat. Commun.* **12** 5896

[66] Cropek C, Ji B, Sarkar A, Wang F, Hussain Syed T, Wei W, Guo S-P and Wang J 2023 Revisiting two thiophosphate compounds constituting d0 transition metal HfP_2S_6 and d10 transition metal α-$Ag_4P_2S_6$ as multifunctional materials for combining second harmonic generation response and photocurrent response *CrystEngComm* **25** 1175–85

[67] Heyd J, Scuseria G E and Ernzerhof M 2003 Hybrid functionals based on a screened Coulomb potential *J. Chem. Phys.* **118** 8207

[68] Houari A and Benissad F 2019 Theoretical Study of Ternary CoSP Semiconductor: A Candidate for Photovoltaic Applications *Adv. Theory Simul.* **2** 1900111

[69] Perdew J P, Burke K and Ernzerhof M 1996 Generalized Gradient Approximation Made Simple *Phys. Rev. Lett.* **77** 3865–8

[70] Heyd J, Scuseria G E and Ernzerhof M 2003 Hybrid functionals based on a screened Coulomb potential *J. Chem. Phys.* **118** 8207–15

[71] Kim S, Lee M, Hong C, Yoon Y, An H, Lee D, Jeong W, Yoo D, Kang Y, Youn Y and Han S 2020 A band-gap database for semiconducting inorganic materials calculated with hybrid functional *Sci. Data* **7** 387

[72] Zhou J, Zhu C, Zhou Y, Dong J, Li P, Zhang Z, Wang Z, Lin Y-C, Shi J, Zhang R, Zheng Y, Yu H, Tang B, Liu F, Wang L, Liu L, Liu G-B, Hu W, Gao Y, Yang H, Gao W, Lu L, Wang Y, Suenaga K, Liu G, Ding F, Yao Y and Liu Z 2022 Composition and phase engineering of metal chalcogenides and phosphorous chalcogenides *Nat. Mater.* 1–9

[73] Xiao Z, Meng W, Wang J, Mitzi D B and Yan Y 2017 Searching for promising new perovskite-based photovoltaic absorbers: the importance of electronic dimensionality *Mater Horiz* **4** 206–16

[74] Green M A, Dunlop E D, Siefer G, Yoshita M, Kopidakis N, Bothe K and Hao X 2023 Solar cell efficiency tables (Version 61) *Prog. Photovolt. Res. Appl.* **31** 3–16

[75] Madsen G K H, Carrete J and Verstraete M J 2018 BoltzTraP2, a program for interpolating band structures and calculating semi-classical transport coefficients *Comput. Phys. Commun.* **231** 140–5

[76] Ricci F, Chen W, Aydemir U, Snyder G J, Rignanese G-M, Jain A and Hautier G 2017 An ab initio electronic transport database for inorganic materials *Sci. Data* **4** 170085

[77] Corbridge D E C 2013 *Phosphorus: chemistry, biochemistry and technology* (Boca Raton: Taylor & Francis)

[78] Davies D W, Butler K T, Jackson A J, Skelton J M, Morita K and Walsh A 2019 SMACT: Semiconducting Materials by Analogy and Chemical Theory *J. Open Source Softw.* **4** 1361

[79] Varley J B, Miglio A, Ha V-A, van Setten M J, Rignanese G-M and Hautier G 2017 High-Throughput Design of Non-oxide p-Type Transparent Conducting Materials: Data Mining, Search Strategy, and Identification of Boron Phosphide *Chem. Mater.* **29** 2568–73

[80] Etourneau J, Portier J and Ménil F 1992 The role of the inductive effect in solid state chemistry: how the chemist can use it to modify both the structural and the physical properties of the materials *J. Alloys Compd.* **188** 1–7

[81] Schnepf R R, Cordell J J, Tellekamp M B, Melamed C L, Greenaway A L, Mis A, Brennecka G L, Christensen S, Tucker G J, Toberer E S, Lany S, Tamboli A C and Tamboli A C 2020 Utilizing Site Disorder in the Development of New Energy-Relevant Semiconductors *ACS Energy Lett.* **5** 2027–41

[82] Kirchartz T and Rau U 2018 What Makes a Good Solar Cell? *Adv. Energy Mater.* **8** 1703385

[83] Zakutayev A, Caskey C M, Fioretti A N, Ginley D S, Vidal J, Stevanović V, Tea E and Lany S 2014 Defect Tolerant Semiconductors for Solar Energy Conversion *J. Phys. Chem. Lett.* **5** 1117–25

[84] Kurchin R C, Gorai P, Buonassisi T and Stevanović V 2018 Structural and Chemical Features Giving Rise to Defect Tolerance of Binary Semiconductors *Chem. Mater.* **30** 5583–92

[85] Brandt R E, Stevanović V, Ginley D S and Buonassisi T 2015 Identifying defect-tolerant semiconductors with high minority-carrier lifetimes: beyond hybrid lead halide perovskites *MRS Commun.* **5** 265–75

[86] Enkovaara J, Rostgaard C, Mortensen J J, Chen J, Dułak M, Ferrighi L, Gavnholt J, Glinsvad C, Haikola V, Hansen H A, Kristoffersen H H, Kuisma M, Larsen A H, Lehtovaara L, Ljungberg M, Lopez-Acevedo O, Moses P G, Ojanen J, Olsen T, Petzold V, Romero N A, Stausholm-Møller J, Strange M, Tritsaris G A, Vanin M, Walter M, Hammer B, Häkkinen H, Madsen G K H, Nieminen R M, Nørskov J K, Puska M, Rantala T T, Schiøtz J, Thygesen K S and Jacobsen K W 2010 Electronic structure calculations with GPAW: a real-space implementation of the projector augmented-wave method *J. Phys. Condens. Matter* **22** 253202

[87] Kuhar K, Crovetto A, Pandey M, Thygesen K S, Seger B, Vesborg P C K, Hansen O, Chorkendorff I and Jacobsen K W 2017 Sulfide perovskites for solar energy conversion applications: computational screening and synthesis of the selected compound $LaYS_3$ *Energy Environ. Sci.* **10** 2579–93

[88] Curtarolo S, Hart G L W, Nardelli M B, Mingo N, Sanvito S and Levy O 2013 The high-throughput highway to computational materials design *Nat. Mater.* **12** 191–201

[89] Kim S, Márquez J A, Unold T and Walsh A 2020 Upper limit to the photovoltaic efficiency of imperfect

crystals from first principles *Energy Env. Sci* **13** 1481–91

[90] Gregoire J M, Zhou L and Haber J A 2023 Combinatorial synthesis for AI-driven materials discovery *Nat. Synth.* 1–12

[91] Ludwig A 2019 Discovery of new materials using combinatorial synthesis and high-throughput characterization of thin-film materials libraries combined with computational methods *Npj Comput. Mater.* **5** 70

[92] Maier W F, Stöwe K and Sieg S 2007 Combinatorial and High-Throughput Materials Science *Angew. Chem. Int. Ed.* **46** 6016–67

[93] Gusmão R, Sofer Z and Pumera M 2019 Metal Phosphorous Trichalcogenides ($MPCh_3$): From Synthesis to Contemporary Energy Challenges *Angew. Chem. Int. Ed.* **58** 9326–37

[94] Liang Z, Yang Z, Dang J, Qi J, Yuan H, Gao J, Zhang W, Zheng H and Cao R 2019 Hollow Bimetallic Zinc Cobalt Phosphosulfides for Efficient Overall Water Splitting *Chem. – Eur. J.* **25** 621–6

[95] Park K, Lee J A, Im H S, Jung C S, Kim H S, Park J and Lee C L 2014 GaP-ZnS pseudobinary alloy nanowires *Nano Lett.* **14** 5912–9

[96] Zhang X, Min K-A, Zheng W, Hwang J, Han B and Lee L Y S 2020 Copper phosphosulfides as a highly active and stable photocatalyst for hydrogen evolution reaction *Appl. Catal. B Environ.* **273** 118927

[97] Quan Z, Hirayama M, Sato D, Zheng Y, Yano T, Hara K, Suzuki K, Hara M and Kanno R 2017 Effect of excess Li_2S on electrochemical properties of amorphous Li_3PS_4 films synthesized by pulsed laser deposition *J. Am. Ceram. Soc.* **100** 746–53

[98] Ito Y, Konishi M, Noi K, Deguchi M, Hayashi A and Tatsumisago M 2018 Sodium thiophosphate electrolyte thin films prepared by pulsed laser deposition for bulk-type all-solid-state sodium rechargeable batteries *J. Ceram. Soc. Jpn.* **126** 475–81

[99] Ito Y, Sakuda A, Ohtomo T, Hayashi A and Tatsumisago M 2014 Li_4GeS_4–Li_3PS_4 electrolyte thin films with highly ion-conductive crystals prepared by pulsed laser deposition *J. Ceram. Soc. Jpn.* **122** 341–5

[100] Willis J, Bravić I, Schnepf R R, Heinselman K N, Monserrat B, Unold T, Zakutayev A, Scanlon D O and Crovetto A 2022 Prediction and realisation of high mobility and degenerate p-type conductivity in CaCuP thin films *Chem. Sci.* **13** 5872–83

[101] Welch A W, Baranowski L L, Zawadzki P, DeHart C, Johnston S, Lany S, Wolden C A and Zakutayev A 2016 Accelerated development of $CuSbS_2$ thin film photovoltaic device prototypes *Prog. Photovolt. Res. Appl.* **24** 929–39

[102] Lund E A, Du H, Hlaing OO W M, Teeter G and Scarpulla M A 2014 Investigation of combinatorial coevaporated thin film Cu_2ZnSnS_4 (II): Beneficial cation arrangement in Cu-rich growth *J. Appl. Phys.* **115** 173503

[103] Musavigharavi P, Kurnia F, Xie L, Park C K Y, Ng Y H, He J, Hart J N and Valanoor N 2021 ZnS-GaP Solid Solution Thin Films with Enhanced Visible-Light Photocurrent *ACS Appl. Energy Mater.* **4** 10756–61

[104] Yim W M 1969 Solid Solutions in the Pseudobinary (III-V)-(II-VI) Systems and Their Optical Energy Gaps *J. Appl. Phys.* **40** 2617–23

[105] Szczuka C, Karasulu B, Groh M F, Sayed F N, Sherman T J, Bocarsly J D, Vema S, Menkin S, Emge S P, Morris A J and Grey C P 2022 Forced Disorder in the Solid Solution Li_3P–Li_2S: A New Class of Fully Reduced Solid Electrolytes for Lithium Metal Anodes *J. Am. Chem. Soc.* **144** 16350–65

[106] Hara T and Akasaki I 2003 Electrical Properties of Sulfur-Doped Gallium Phosphide *J. Appl. Phys.* **39** 285–9

[107] Siol S, Dhakal T P, Gudavalli G S, Rajbhandari P P, DeHart C, Baranowski L L and Zakutayev A 2016 Combinatorial Reactive Sputtering of In_2S_3 as an Alternative Contact Layer for Thin Film Solar Cells *ACS Appl. Mater. Interfaces* **8** 14004–11

[108] Crovetto A, Unold T and Zakutayev A 2023 Is $Cu_{3-x}P$ a Semiconductor, a Metal, or a Semimetal? *Chem. Mater.* **35** 1259–72

[109] Baranowski L L, Zawadzki P, Christensen S, Nordlund D, Lany S, Tamboli A C, Gedvilas L, Ginley D S, Tumas W, Toberer E S and Zakutayev A 2014 Control of Doping in Cu_2SnS_3 through Defects and Alloying *Chem. Mater.* **26** 4951–9

[110] Scragg J J, Ericson T, Fontané X, Izquierdo-Roca V, Pérez-Rodríguez A, Kubart T, Edoff M and Platzer-Björkman C 2014 Rapid annealing of reactively sputtered precursors for Cu_2ZnSnS_4 solar cells *Prog. Photovolt. Res. Appl.* **22** 10–7

[111] Crovetto A, Adamczyk J M, Schnepf R R, Perkins C L, Hempel H, Bauers S R, Toberer E S, Tamboli A C, Unold T and Zakutayev A 2022 Boron Phosphide Films by Reactive Sputtering: Searching for a p-Type Transparent Conductor *Adv. Mater. Interfaces* **9** 2200031

[112] Scragg J J, Dale P J, Colombara D and Peter L M 2012 Thermodynamic aspects of the synthesis of thin-film materials for solar cells. *Chemphyschem Eur. J. Chem. Phys. Phys. Chem.* **13** 3035–46

[113] Crovetto A, Ottsen T S, Stamate E, Kjær D, Schou J and Hansen O 2016 On performance limitations and property correlations of Al-doped ZnO deposited by radio-frequency sputtering *J. Phys. Appl. Phys.* **49** 295101

[114] Crovetto A, Nielsen R, Stamate E, Hansen O, Seger B, Chorkendorff I and Vesborg P C K 2019 Wide Band Gap Cu_2SrSnS_4 Solar Cells from Oxide Precursors *ACS Appl. Energy Mater.* **2** 7340–4

[115] Comparotto C, Ström P, Donzel-Gargand O, Kubart T and Scragg J J S 2022 Synthesis of $BaZrS_3$ Perovskite Thin Films at a Moderate Temperature on Conductive Substrates *ACS Appl. Energy Mater.*

[116] Yu Z, Wei X, Zheng Y, Hui H, Bian M, Dhole S, Seo J-H, Sun Y-Y, Jia Q, Zhang S, Yang S and Zeng H 2021 Chalcogenide perovskite BaZrS3 thin-film electronic and optoelectronic devices by low temperature processing *Nano Energy* **85** 105959

[117] Martinho F, Hajijafarassar A, Lopez-Marino S, Espíndola-Rodríguez M, Engberg S, Gansukh M, Stulen F, Grini S, Canulescu S, Stamate E, Crovetto A, Vines L, Schou J and Hansen O 2020 Nitride-Based Interfacial Layers for Monolithic Tandem Integration of New Solar Energy Materials on Si: The Case of CZTS *ACS Appl. Energy Mater.* **3** 4600–9

[118] Yan C, Huang J, Sun K, Johnston S, Zhang Y, Sun H, Pu A, He M, Liu F, Eder K, Yang L, Cairney J M, Ekins-Daukes N J, Hameiri Z, Stride J A, Chen S, Green M A and Hao X 2018 Cu_2ZnSnS_4 solar cells with over 10% power conversion efficiency enabled by heterojunction heat treatment *Nat. Energy* **3** 764–72

[119] Succi M, Canino R and Ferrario B 1985 Atomic absorption evaporation flow rate measurements of alkali metal dispensers *Vacuum* **35** 579–82